Published in final edited form as:

Hypertension. 2016 June ; 67(6): 1298–1308. doi:10.1161/HYPERTENSIONAHA.116.07367.

PPARγ Level Contributes to Structural Integrity and Component Production of Elastic Fibers in the Aorta

Haw-Chih Tai, MS[1,2], **Pei-Jane Tsai, PhD**[3], **Ju-Yi Chen, MD, PhD**[1,2,4], **Chao-Han Lai, MD, PhD**[1,2,5], **Kuan-Chieh Wang, PhD**[2,6], **Shih-Hua Teng, PhD**[7], **Shih-Chieh Lin, PhD**[8], **Alice Y. W. Chang**[8], **Meei-Jyh Jiang, PhD**[2,9], **Yi-Heng Li, MD, PhD**[2,4], **Hua-Lin Wu, PhD**[2,6], **Nobuyo Maeda, PhD**[10], and **Yau-Sheng Tsai, PhD**[1,2,11]

[1]Institute of Clinical Medicine, National Cheng Kung University, Tainan, Taiwan, ROC

[2]Cardiovascular Research Center, National Cheng Kung University, Tainan, Taiwan, ROC

[3]Department of Medical Laboratory Science and Biotechnology, National Cheng Kung University, Tainan, Taiwan, ROC

[4]Department of Internal Medicine, National Cheng Kung University Hospital, College of Medicine, National Cheng Kung University, Tainan, Taiwan, ROC

[5]Department of Surgery, National Cheng Kung University Hospital, College of Medicine, National Cheng Kung University, Tainan, Taiwan, ROC

[6]Department of Biochemistry and Molecular Biology, National Cheng Kung University, Tainan, Taiwan, ROC

[7]Graduate Institute of Biomedical Sciences, Chang Gung University, Taoyuan, Taiwan, ROC

[8]Department of Physiology, National Cheng Kung University, Tainan, Taiwan, ROC

[9]Department of Cell Biology and Anatomy, National Cheng Kung University, Tainan, Taiwan, ROC

[10]Department of Pathology and Laboratory Medicine, University of North Carolina at Chapel Hill, Chapel Hill, NC, USA

[11]Research Center of Clinical Medicine, National Cheng Kung University Hospital, College of Medicine, National Cheng Kung University, Tainan, Taiwan, ROC

Abstract

Loss of integrity and massive disruption of elastic fibers are key features of abdominal aortic aneurysm (AAA). Peroxisome proliferator-activated receptor γ (PPARγ) has been shown to attenuate AAA through inhibition of inflammation and proteolytic degradation. However, its involvement in elastogenesis during AAA remains unclear. PPARγ was highly expressed in human AAA within all vascular cells, including inflammatory cells and fibroblasts. In the aortas of transgenic mice expressing PPARγ at 25% normal levels (*Pparg*$^{C/-}$ mice), we observed the

Address Correspondence to: Yau-Sheng Tsai, 1 University Road, National Cheng Kung University, Tainan 701, Taiwan. Phone: 886-6-2353535-4242; Fax: 886-6-2758781; yaustsai@mail.ncku.edu.tw.

Disclosures

None.

fragmentation of elastic fibers and reduced expression of vital elastic fiber components of elastin and fibulin-5. These were not observed in mice with 50% normal PPARγ expression (*Pparg*$^{+/-}$ mice). Infusion of a moderate dose of angiotensin II (AngII) (500 ng/kg/min) did not induce AAA but *Pparg*$^{+/-}$ aorta developed flattened elastic lamellae, while *Pparg*$^{C/-}$ aorta showed severe destruction of elastic fibers. After infusion of AngII at 1000 ng/kg/min, 73% of *Pparg*$^{C/-}$ mice developed atypical suprarenal aortic aneurysms: superior mesenteric arteries were dilated with extensive collagen deposition in adventitia and infiltrations of inflammatory cells. Although matrix metalloproteinase inhibition by doxycycline somewhat attenuated the dilation of aneurysm, it did not reduce the incidence nor elastic lamella deterioration in AngII-infused *Pparg*$^{C/-}$ mice. Furthermore, PPARγ antagonism down-regulated elastin and fibulin-5 in fibroblasts, but not in vascular smooth muscle cells. Chromatin immunoprecipitation assay demonstrated PPARγ binding in the genomic sequence of fibulin-5 in fibroblasts. Our results underscore the importance of PPARγ in AAA development though orchestrating proper elastogenesis and preserving elastic fiber integrity.

Keywords

PPARγ; elastic lamella; aneurysm; fibulin-5; fibroblasts

Introduction

While open surgical or endovascular repair procedures have reduced the mortality of ruptured abdominal aortic aneurysm (AAA) in the past decade,[1] no effective pharmacological treatment has been conducted to inhibit the progression and rupture of human AAAs. Although medical management for hypertension and hyperlipidemia reveals potential benefits for lowering the growth rate of AAA,[2] directly targeting vessel health is urgently needed. To this end, factors and cell types that are involved in the development of aneurysm need revisited.

Loss of integrity and massive disruption of elastic architecture are key features of structural changes in AAA.[3] Elastic fiber is formed by initial synthesis of soluble precursor tropoelastin and later maturation by crosslinking of fibulins (fibulin-4 and fibulin-5) and fibrillins (fibrillin-1 and fibrillin-2) scaffold with the elastin core.[4] In contrast, extensive infiltration of macrophages and lymphocytes increases the local expression of pro-inflammatory cytokines and triggers production of elastolytic proteases. Elastic fibers are degraded by matrix metalloproteinases (MMP-2, MMP-9, MMP-7 and MMP-12) and cysteine proteinases (cathepsin S and cathepsin K).[5] Aortic fibroblasts in AAA have not been well discussed, but they are documented within the media and adventitia of aneurysm, and express higher levels of several collagens and elastin.[6] Thus, aortic fibroblasts may actively participate in elastic fiber turnover particularly when vascular smooth muscle cells (VSMCs) and elastic fiber components are compromised in AAA.

PPARγ has been shown to protect from vascular diseases through its anti-inflammatory effect. PPARγ activation in inflammatory cells reduces production of TNF-α, IL-1β and IL-6.[7] PPARγ activation in VSMCs suppresses MMP-9 expression and collagen over-

production.[8, 9] Treatment with PPARγ agonists protects aorta against nicotine-induced calcification and elastic fiber fragmentation,[10] and reduces the development and rupture of AngII-induced AAA.[11] On the other hand, loss of PPARγ in VSMCs promotes aortic dilatation and elastin degradation in $CaCl_2$-induced AAA.[12] While these findings indicate a critical role of PPARγ in reduction of inflammation and elastic fiber degradation in AAA, several questions remain unsolved. First, the role of PPARγ in elastic fiber component production remains unclear. Second, the involvement of adventitial fibroblasts in PPARγ protective effect is lacking. Third, although PPARγ gene polymorphism is associated with the incidence and growth of AAA,[13] the threshold levels of PPARγ to maintain integrity and prevent from AAA are not known.

In this study, we have tested our hypothesis that PPARγ plays key roles in maintenance of the elastic fiber integrity and prevention of AAA in response to exogenous stimuli, such as increased AngII. We took advantage of mice genetically altered to have different levels of PPARγ expression from 25% to 100%, and unveiled that fibroblasts express high levels of PPARγ in AAA and directly contribute to increased elastogenesis. When infused with AngII, mice with 25% PPARγ expression develop severely dilated suprarenal aneurysms involving roots of celiac artery (CA) and superior mesenteric artery (SMA). Our data underscore the importance of PPARγ in orchestrating proper elastogenesis and preserving elastic fiber integrity during AAA development.

Methods

Expanded Materials and Methods are available in the online-only Data Supplement.

Human Tissue Procurement

Human AAA samples were collected during open surgical repair of AAA. Samples from two patients were used for immunohistochemical staining. The specificity of primary antibody was confirmed by negative control procedures which gave consistently negative results (Figure S1). One patient had hypertension and the other had diabetes mellitus, and the diameters of infrarenal AAAs were 7.4 cm and 8 cm, respectively. Sections of normal human aorta, purchased from Origene, were obtained from a 57-year-old male with heart valve disorder. Sample diagnosis from pathology verification was non-tumor structures and within normal limits. The use of human samples was approved by the Institutional Review Board of National Cheng Kung University Hospital.

Mice

Experimental mice were F1 littermates from the mating of $Pparg^{C/+}$ mice on a C57BL/6J background with $Pparg^{+/-}$ mice on a 129S6 background.[14] Two to three-month-old male $Pparg^{+/+}$, $Pparg^{+/-}$ and $Pparg^{C/-}$ littermates were used in all experiments. The following groups were studied: (1) No AngII infusion in $Pparg^{+/+}$, $Pparg^{+/-}$ and $Pparg^{C/-}$ mice, (2) AngII (500 ng/kg/min) infusion in $Pparg^{+/+}$, $Pparg^{+/-}$ and $Pparg^{C/-}$ mice, (3) AngII (1000 ng/kg/min) infusion in $Pparg^{+/+}$, $Pparg^{+/-}$ and $Pparg^{C/-}$ mice, (4) AngII (1000 ng/kg/min) infusion + doxycycline (30 mg/kg/day) administration in $Pparg^{C/-}$ mice. All animal studies

were performed according to protocols approved by the Institutional Animal Care and Use Committee of National Cheng Kung University.

Morphological Analysis of Aorta

The elastic fiber network was evaluated in the paraffin-embedded aortic section (5 μm) with Verhoeff's stain (Sigma-Aldrich). Thickness of elastic lamella was measured by ImageJ software (NIH), and the average was based on > 24 randomly selected elastic lamellae from 6 different cross-sectional fields per aorta. Waviness of elastic lamellae was graded on a scale from 1 to 5 in eight to ten non-overlapping fields of medial section: 1 (<20% of the waviness of a normal lamella), 2 (20~40% waviness), 3 (40~60% waviness), 4 (60~80% waviness), and 5 (>80% waviness); and the average of waviness score was presented.

Severity Grading of Aneurysm

The severity grading of mouse AAA was adapted according to the classification by Daugherty et al.[15] We defined our severity grading of AAA by the pronounced form and its covered area of the aorta. Severity of aneurysm was graded on a scale from 0 to 4: 0 (no dilation in suprarenal aorta), 1 (dilation only in suprarenal aorta), 2 (dilation of suprarenal aneurysm that contains the root of CA and SMA), 3 (pronounced dilated aneurysm from suprarenal AA to SMA), 4 (rupture of aorta or death).

Data Analysis

Values are reported as mean ± SEM. Statistical analyses were conducted by Student's *t*-test, one-way ANOVA followed by Tukey HSD multiple comparison test, or two-way ANOVA with treatment and genotype as factors. Differences were considered to be statistically significant at $P<0.05$.

Results

Upregulation of PPARγ in both Human and Mouse AAA

To evaluate the involvement of PPARγ in AAA, we first determined the expression of PPARγ in human AAA by immunohistochemistry. Normal human aortic samples scarcely expressed PPARγ (Figure 1A~B). Some PPARγ-positive cells with a high nuclear-cytoplasmic ratio were present in the adventitia (Figure 1C). In human AAA sections, the intima was thickened with typical atherosclerotic changes, while media was significantly thinned. PPARγ expression was markedly increased within the atheroma under the fibrous caps as well as deeper near the media (Figure 1D). Within the media of aneurysm, PPARγ was increased in elongated cells with tapering ends, the characteristics of VSMCs (Figure 1E). Within the adventitia of aneurysm, PPARγ was expressed markedly in cells with a high nuclear-cytoplasmic ratio with the characteristics of inflammatory cells (black arrows, Figure 1F). The bulk of inflammatory cells with high nuclear-cytoplasmic ratio in AAA have been reported as $CD3^+$ T lymphocytes and $CD19^+$ B lymphocytes.[16] Consistently, only a small portion of inflammatory cells was positive for CD68 staining (Figure S2). PPARγ was also expressed in endothelial cells associated with vasa vasorum, and occasionally in spindle shaped cells indicative of fibroblasts (white arrowheads, Figure 1F).

PPARγ expression in the normal abdominal aorta (AA) of wild-type (WT) mice was sparsely detected in VSMCs (Figure 1G-1I). While AAA occurs very rarely in WT mice even after infusion of AngII at 1000 ng/kg/min for 4 weeks, we observed in one of the treated mice a large bulge of upper suprarenal aorta with a dissecting AAA histology (Figure S3) similar to those documented previously.[17] PPARγ expression was markedly elevated compared to the intact vessels particularly in which the tunica media is torn and bordered by the organizing intramural hematoma (Figure 1J and 1K), as well as in the adventitia (Figure 1L). Consistent with that in human AAA, PPARγ was mainly expressed in inflammatory cells with a high nuclear-cytoplasmic ratio in the luminal surface of vessels and in adventitia. PPARγ was also expressed in cells with a spindle shape present in relatively intact medial layers (Figure 1K) and in adventitia (Figure 1L), respectively representing VSMCs and fibroblasts. These results indicate PPARγ is upregulated in all vascular cell types in atherosclerosis-associated AAA in humans as well as in AngII-induced AAA in mice.

Increased Elastic Fiber Fragmentation in *Pparg*$^{C/-}$ Aorta

To examine the functional significance of PPARγ upregulation in AAA development, we took advantage of mice with genetic reduction in the *Pparg* gene expression down to 25% normal (*Pparg*$^{C/-}$) generated by crossing mice having a PPARγ deletion allele (*Pparg*$^{+/-}$) with mice bearing an allele of *c-fos* ARE sequence inserted into the PPARγ 3′-UTR region (*Pparg*$^{C/+}$).[14] mRNA and protein levels of PPARγ in the descending aorta of *Pparg*$^{C/-}$ mice were decreased to 40% and 29% of the WT levels, respectively (Figure S4A and Figure 2A); and the reduction was confirmed by the immunohistochemical staining (Figure S4B). In addition, the ratio to PPARγ level of Ser82 phosphorylation, which is known to inhibit its transactivation, was higher in *Pparg*$^{C/-}$ aorta (Figure S5), suggesting that PPARγ activity may be even repressed in *Pparg*$^{C/-}$ aorta. *Pparg*$^{C/-}$ mice have normal plasma cholesterol levels, but, consistent with our previous findings,[18] they are hypertensive showing higher systolic blood pressure (BP) in both light and dark cycles during the telemetric monitoring and by a tail-cuff method (Figure 2B and 2C). No gross abnormality in the vascular dimensions was present in *Pparg*$^{C/-}$ mice (Table S1 and Figure S4C). However, under light microscopic examination, occasional breaks of medial elastic fibers were noted in the closer look of the aortas of *Pparg*$^{C/-}$ mice (Figure 2D). Expression of genes coding for elastin degradation enzymes MMP-9 and cathepsin S (*Ctss*) was increased in *Pparg*$^{C/-}$ aorta (Figure 2E). MMP-9, but not cathepsin S, protein level was elevated in *Pparg*$^{C/-}$ aorta, particularly in the medial layer near luminal side (Figure 2A and 2F). We also found a significantly increased expression of TNF-α and F4/80 (*Adgre1*) and a trend toward increased expression of IL-1β in *Pparg*$^{C/-}$ aorta (Figure 2G). These results suggest that the elastic fiber fragmentation in *Pparg*$^{C/-}$ aorta is associated with increased elastolytic enzymes and inflammation in the aorta.

Reduced Production of Elastic Fiber Components in *Pparg*$^{C/-}$ Aorta

Defective elastic fiber formation can also lead to its fragmentation. We therefore examined elastic fiber components by immunoblotting in the soluble fraction of aortic lysate, which reveals free monomers before assembly into mature fibers. In *Pparg*$^{C/-}$ aorta, tropoelastin level was tended to be less and fibulin-5 level was significantly reduced (Figure 2H). The levels of collagen type I and fibulin-4 were not different between genotypes. To determine

the insoluble fraction of aortic lysate, which directly reflects the functional scaffold of mature fibers, we applied liquid chromatography (LC)/mass spectrometer (MS)-based label-free quantitative proteomic analysis. Among 376 identified proteins from insoluble pellets of aortic lysates, 37 proteins were above the identity threshold (Table S2). Many of these proteins are vital for ECM organization and elastic fiber assembly in these 37 proteins (Table 1). Interestingly, levels of fibulin-5 (0.61), elastin (0.82), fibrillin-1 (0.84) and lysyl oxidase homolog 1 (Loxl1; 0.87) were decreased, whereas the levels of collagen alpha-1(I) (1.00), alpha-2(I) (1.09), and tubulin alpha-1A (1.00) were not altered in *Pparg*$^{C/-}$ aorta.

At mRNA levels, *Pparg*$^{C/-}$ aortas have significantly reduced expression of *Eln*, *Fbln4*, *Fbln5*, and a trend toward decreased *Fbn1* expression (Figure 2I). In contrast, expression of *Eln*, *Fbln4*, *Fbln5*, and *Mmp9* was not significantly changed in *Pparg*$^{+/-}$ aorta (Figure S6). Taken together, these results suggest that severe PPARγ hypomorph itself, without advanced stimulations, reduces expression of elastic fiber components, which may also contribute to the structural change of mature elastic fibers.

Synergistic Effect of AngII and PPARγ Deficiency on Elastic Fiber Disruption

To test whether *Pparg* level may mark the aorta for its susceptibility to exogenous insult-induced injuries, we infused AngII into mice at a moderate dose of 500 ng/kg/min for 4 weeks. AngII infusion significantly increased systolic BP in both WT and *Pparg*$^{C/-}$ mice by approximately 20 mmHg (P<0.001 by two-way ANOVA, Figure 3A and Figure S7) compared to untreated mice measured concurrently (Figure 2B). PPARγ genotype had a significant effect on elevation of systolic BP (P<0.01) without the interaction between AngII and genotype. All AngII-infused mice were fed a cholesterol-enriched western diet, but neither atherosclerotic lesions nor aneurysms developed in any of these mice. Elastin staining of *Pparg*$^{+/+}$ thoracic aorta (TA) and AA showed organized, wavy and consistently thickened elastic lamella arrangement. Although *Pparg*$^{+/-}$ TA and AA maintained relatively intact fiber structures, elastic lamellae in both of them became thinner, flattened and lost the wavy feature (Figure 3B and 3C). Flattened elastic lamellae were also observed in *Pparg*$^{C/-}$ TA and AA. Additionally, while the integrity of elastic lamellae was preserved in *Pparg*$^{C/-}$ TA, elastic lamellae in *Pparg*$^{C/-}$ AA exhibited severe destruction with extensive inconsistency in thickness and fragmentation into short, thin and fragile segments. Quantitation revealed a marked reduction of elastic fiber consistency and an increase of breaks in the AA of *Pparg*$^{C/-}$ mice, but the fibers remained normal in *Pparg*$^{+/-}$ mice (Figure 3C and Table S3). Thus, our data suggests that 50% reduction in the PPARγ expression can still maintain the consistency of elastic fiber in response to a moderate dose of AngII, but further reduction will affect structural integrity.

At the molecular level, we found that PPARγ deficiency in combination with AngII infusion upregulated expressions of aortic TNF-α, IL-1β, MCP-1 (*Cc12*) and F4/80 (*Adgre1*; Figure 3D), as well as a series of elastin-degradation enzymes, including MMP-7, MMP-9 and cathepsin S (*Ctss*; Figure 3E). Gelatin zymography confirmed elevated MMP-9, but normal MMP-2, activity in the AA of AngII-infused *Pparg*$^{C/-}$ mice (Figure 3F). However, MMP-9 activity remained comparable in the TA of *Pparg*$^{C/-}$ mice. Thus, reduction of PPARγ levels renders the aorta susceptible to AngII-induced inflammation and elastic fiber disruption. In

AngII-induced mouse AAA, oxidative stress is critical in the regulation of pathogenic events.[19] Accordingly, we examined expression of pro-oxidant (*Cyba*, *Ncf1*, and *Ncf2*) and anti-oxidant enzymes (*Sod1* and *Cat*) in $Pparg^{+/+}$ and $Pparg^{C/-}$ aorta (Figure S8). Analysis of results with two-way ANOVA showed that AngII (500 ng/kg/min) has significant effects on expression of NADPH oxidase components (*Cyba*, *Ncf1*, and *Ncf2*) and superoxide dismutase 1 (*Sod1*). However, no PPARγ genotype effect was found in the expression of *Cyba*, *Ncf1*, *Ncf2*, *Sod1*, and *Cat* (catalase). These results suggest that although oxidative stress is critical in AngII-induced AAA, accelerated development of AAA seen in $Pparg^{C/-}$ mice is independent of oxidative stress.

Atypical AAA with Severe SMA Dilation in High-Dose AngII-Infused $Pparg^{C/-}$ Mice

A higher dose of AngII (1000 ng/kg/min) infusion for 4 weeks is commonly used for aneurysm induction in rodents.[20] At this dose, BPs of mice increased further as summarized in Figure S7. After 4 weeks of infusion, 1 of 11 $Pparg^{+/+}$ mice developed bulbous suprarenal aneurysm in the left side above the celiac artery branch (Figure S3). In a marked contrast, 8 of 11 (73%) $Pparg^{C/-}$ mice developed dilated suprarenal aneurysms (Figure 4A~4C). The aneurysms in $Pparg^{C/-}$ mice were, however, atypical and the enlargement was towards the ventral side and restricted to a narrow region involving roots of celiac artery (CA) and superior mesenteric artery (SMA). Such profound SMA dilatation was not present in the aorta of $Pparg^{+/+}$ mice, and only 1 of 5 $Pparg^{+/-}$ mice developed similar but smaller suprarenal aneurysms compared to $Pparg^{C/-}$ mice. We monitored the time course of AAA *in vivo* by ultrasound on the mice 2 and 3 weeks post-AngII pump (1000 ng/kg/min) implantation. The enlargement of the suprarenal aortic lumen of $Pparg^{C/-}$ mice was observed at 2 weeks (33%), and continuously increased at 3 weeks (66%). Suprarenal aortic lumen diameter was enlarged to 1.64±0.29 mm in $Pparg^{C/-}$ mice compared to 1.12±0.05 mm in $Pparg^{+/+}$ mice at the 3-week time point (Figure S9).

Histologically, upper portion of the aneurysm (Figure 4D) illustrates the dilatation at the branching point of CA in which elastic lamellae of the artery were severely destroyed, although their reminiscence clearly demarks the continuity. Intimal thickening was characterized by the presence of both VSMCs and inflammatory cells, while adventitial hyperplasia was marked with extensive collagen deposition and inflammatory cells (Figure 4D). Similar abnormalities were observed near the ostium of SMA (Figure 4E). Neither signs of truncation of tunica media nor intramural hematoma, such as illustrated in the AAA of WT mice in Figure S3, were detected in any of the aneurysms of $Pparg^{C/-}$ mice.

Both the arterial lumen size and wall thickness of $Pparg^{C/-}$ SMA were grossly increased (Figure S10A and S10B). Destruction of medial elastic lamellae (Elastin stain) and compensatory deposition of collagen (PS red) were found in the hypertrophic adventitia of $Pparg^{C/-}$ SMA (Figure S10C). Immunohistochemical staining showed that the smooth muscle density (SMactin) was decreased in the medial layer. Interestingly, the dilated adventitial region contained predominantly fibroblasts (fibroblast activation protein, FAP) (Figure S10D), and showed a dramatic increase of Ki-67-positive signal (Figure S11), suggesting that these FAP-positive cells are highly proliferative. Additionally extensive macrophage infiltration (MOMA-1) was evident in the outer layer of adventitia (Figure

S10D). MMP-9 level was dramatically augmented in the medial to adventitial layer of *Pparg*$^{C/-}$ SMA.

No Change of Aneurysm Incidence by MMP Inhibition

To examine whether MMP activity is crucial for the onset of *Pparg*$^{C/-}$ AAA, a broad-spectrum MMP inhibitor doxycycline (DOX) was administrated in AngII-infused *Pparg*$^{C/-}$ mice. DOX (30 mg/kg/day) suppressed aortic MMP-9 activity in *Pparg*$^{C/-}$ mice (Figure 5A). However, although DOX treatment attenuated SMA dilation and the diameter of aneurysmal dilatations in *Pparg*$^{C/-}$ mice (Figure 5B and 5C), it did not reduce the severity and incidence of aneurysm (Figure 5D and 5E; P=0.65 for incidence with Chi square test, P=0.53 even after including earlier 8/11). Moreover, DOX treatment did not ameliorate profound deterioration and fragile elastic lamellae in the lower AA of *Pparg*$^{C/-}$ mice (Figure 5F), as illustrated by the parameters of AA elastic fiber impairments (Figure 5G). These results imply that the reduction of fiber component synthesis in *Pparg*$^{C/-}$ aorta plays a key role in the initiation of AAA, the pathology of which is significantly enhanced by the increased MMP expression associated with inflammation.

PPARγ Antagonism Inhibits Expression of Elastic Fiber Components in Fibroblasts

In *Pparg*$^{C/-}$ aorta, both *Eln* and *Fbln5* expression was reduced even without AngII infusion (Figure 2I). Since inflammation has been suggested to affect elastin expression,[21] we next asked whether PPARγ antagonism or TNF-α elevation inhibits the expression of *Eln* and *Fbln5* in aortic smooth muscle cells (ASMCs) and in fibroblasts. Treatments of rat and human ASMCs with neither GW9662 nor TNF-α altered the expression of *Eln* and *Fbln5* (Figure 6A and Figure S12). In a marked contrast, GW9662 significantly suppressed expression of *Eln* and *Fbln5* in mouse embryonic fibroblasts (MEFs) (Figure 6B). TNF-α significantly suppressed *Eln* expression, and tended to decrease *Fbln5* expression. PPARγ knockdown in MEFs reduced expression of both *Eln* and *Fbln5* (Figure 6C), indicating that low expression of PPARγ is sufficient to affect the expression of these genes in MEFs. Although PPARγ knockdown in human aortic adventitial fibroblasts (HAoAFs) significantly reduced expression of *FBLN5*, it did not alter *ELN* (Figure 6D). These results suggest that PPARγ also has a regulatory role in the expression of fibulin-5 in HAoAFs.

Searching for previously reported chromatin immunoprecipitation (ChIP)-sequencing data,[22] we found three potential PPARγ binding sites in *Fbln5*, but none in *Eln*, *Fbln4* and *Fbn1*. ChIP-PCR in MEFs showed that PPARγ bound to *Fbln5* after treatment of PPARγ agonist rosiglitazone, whereas GW9662 abrogates the binding of PPARγ to *Fbln5* (Figure 6E), indicating that *Fbln5* is the direct target of PPARγ. No interaction between PPARγ and *Eln* was identified.

Finally, expression of *Mmp9* in rat ASMCs was induced 2 to 3-fold by GW9662 alone, and 2-fold by TNF-α (Figure 6F; P<0.001 for GW9662 and P<0.01 for TNF-α by two-way ANOVA). In contrast, expression of *Mmp9* in MEFs was induced 20-fold by TNF-α, but not affected by GW9662 (Figure 6G). Taken together, these results demonstrate a direct regulatory role of PPARγ in the expression of elastic fiber components, which takes place

mainly in fibroblasts. Inflammation further contributes to elastic fiber deterioration in *Pparg*$^{C/-}$ aorta via the induction of *Mmp9* in the vascular cells.

Discussion

Our study demonstrated the dosage effect of PPARγ on the elastic fiber integrity and that adequate PPARγ level is vital for production of elastic fiber components. Qualitatively, healthy elastic lamellae show wavy, curl feature and consistency in thickness, whereas poor ones become flattened and irregularly thickened. We observed a significant loss of waviness and a decrease of fiber thickness in moderate-dose AngII-infused *Pparg*$^{+/-}$ aortas, despite they retained structural integrity without fiber fragmentation. PPARγ expression down to 25% further induces thickness inconsistency and fiber breaks in *Pparg*$^{C/-}$ aortas. Thus a critical amount of PPARγ for maintaining normal elastic waviness is above 50%, whereas the threshold level for structure deterioration is between 25% and 50%. These findings suggest that loss of elastic fiber waviness is a hallmark of early elastic fiber defect and likely attributable to PPARγ insufficiency.

Our LC/MS-based label-free quantitative proteomic analysis of mature elastic fiber components in the insoluble ECM fraction showed that fibulin-5, elastin, fibrillin-1 and Loxl1, all vital components for elastic fiber assembly, are down-regulated in *Pparg*$^{C/-}$ aorta. During elastic fiber assembly, elastin is transported to extracellular space, interacts with fibulin-5, and binds to fibrillin-1-formed microfibril scaffold. Lysyl oxidase and its gene family, including Loxl1, catalyzes cross-linking of elastin core and microfibril scaffold, forming the functional fiber unit.[4, 23] Both deficiencies in fibulin-5 and fibrillin-1 cause significant fragmentation and disorganization of elastic fibers, whereas Loxl1 deficiency leads to imprecise and lower cross-linking of elastic fibers.[24] Thus, the reduction of these elastic fiber components suggests a direct regulatory role of PPARγ in elastic fiber production and assembly.

Infusion of AngII raises BP in mice and a high-dose treatment provides an established model of AAA by hypertension.[25] Independently, a decreased PPARγ expression in mice results in increased BP,[18] and *Pparg*$^{C/-}$ mice consistently have 7~18 mmHg higher basal as well as both moderate and high-dose AngII-infused BP than WT mice. Thus increased aortic wall stress likely contributes to higher AAA incidence of *Pparg*$^{C/-}$ mice treated with a high-dose AngII. However, high BP may not account for all the aspects of AAA development, since *Pparg*$^{C/-}$ mice exhibit loss of elastic fiber integrity even without AngII stimulation. *Pparg*$^{C/-}$ mice are more prone to develop aneurysms likely because of a combination of increased BP and weak elastic tissues. Supporting this, Kanematsu et al have previously shown that co-treatment of AngII and beta-aminopropionitrile, a lysyl oxidase inhibitor, markedly increased AAA incidence in mice, suggesting that induced degeneration of elastic lamellae enhances the aortic aneurysm incidence caused by hypertension.[26]

The morphologic features of the AngII-induced AAA in *Pparg*$^{C/-}$ mice, however, differ in some specific manners from those typically described on AAA in rodents including those described by Kanematsu et al.[17, 26] Firstly, no medial rupture was present in *Pparg*$^{C/-}$ aorta, despite increased fragmentation of elastic lamellae. Perhaps enhanced fibroblast

proliferation and collagen synthesis in the adventitia acts to protect the wall against rupture dampening the stress in the media. Secondly, aortic dilatation in *Pparg*$^{C/-}$ mice appears to be initiated near the branching of CA and SMA, and involves the severe dilatation and adventitial fibrosis of these arteries. The turbulence of blood flow is likely to be quite high at this location since CA and SMA are the major branches of AA. Another consideration is that VSMCs of CA and SMA are methothelium origin,[27] while aortic VSMCs are dorsal somite origin.[28] Being composed of two different types of embryonic cells may render the ostia more susceptible to injury. Additionally, PPARγ dependency in the cells of two different origins may also differ. Finally, a recent report by Davis *et al* addressed AngII-induced SMA aneurysm in mice lacking LRP1 specifically in smooth muscle cells (smLRP1$^{-/-}$).[29] These mice showed dilated SMA with severe adventitial and intimal thickenings similar to what we observed in *Pparg*$^{C/-}$ mice. The difference was that the dilatation in smLRP1$^{-/-}$ mice appears to be restricted to SMA, while the dilatation in *Pparg*$^{C/-}$ mice also involves CA and aorta. We note that there is a potential LRP1/PPARγ interaction,[30] and the *LRP1* gene has a PPARγ binding site.[31]

Immediate backup by *de novo* generation of components for fiber production and assembly is a critical process in forming a functional fiber unit during AAA development. However, overwhelming degradation and massive destruction of elastic fiber can mask the underlying defects of elastic fiber production. For instance, the upregulation of elastolytic MMP-9 and cathepsin S was profound in AngII infused-*Pparg*$^{C/-}$ aortas. DOX administration prior to AAA induction has been shown to reduce the incidence and dilation of AAA efficiently through inhibiting MMP in elastase-induced wild-type or hypercholesterolemic AngII-infused mice.[32, 33] However, DOX did not regress or prevent the progression of established AngII-induced AAAs.[34] Our study showed that DOX pre-treatment attenuated aneurysmal dilation, but it did not reduce the incidence of AAA in *Pparg*$^{C/-}$ mice. Importantly, DOX did not ameliorate profound deterioration of elastic lamellae in *Pparg*$^{C/-}$ AA. Thus, attenuation of AAA incidence in the aorta by DOX appears to require intact elastogenesis machinery, whereas it is not effective in the elastogenesis-defective aorta. Although proteinases other than MMPs mediating this profound destruction cannot be excluded, the negative effect of DOX on *Pparg*$^{C/-}$ AAA is likely due to pre-exited defects in elastic fiber integrity and elastogenesis. The controversial effects of DOX in attenuating AAA growth in clinical studies[35, 36] could also be related to the individual variations in elastogenesis machinery.

The role of VSMCs in vascular wall integrity and the significance of VSMC loss in AAA development have been well documented.[37] A loss of PPARγ in VSMCs has been shown to promote aortic dilatation and elastin degradation in $CaCl_2$-induced AAA, indicating a critical role of PPARγ in attenuation of inflammation and elastic fiber degradation in VSMCs during AAA. In contrast, fibroblast, another actively participant in the structural remodeling of AAA, has not gained much attention to date. Despite that the lack of cell selectivity in *Pparg*$^{C/-}$ model is a limitation in dissecting the cell-specific role of PPARγ level, our current results strongly suggest an important role of fibroblast PPARγ in AAA development. For example, we found that one of the predominant cell types in both human and mouse AAA lesions expressing high-level of PPARγ had fibroblast-like features. In addition, a fibroblast marker, FAP, was substantially elevated in the dilated adventitia of *Pparg*$^{C/-}$ aneurysm. FAP is expressed by activated (highly proliferative) fibroblasts in

epithelial tumor stroma, arthritis, and wound healing.[38] Although we cannot determine the origin of these FAP-positive cells, a dramatic increase of Ki-67-positive signal in the dilated adventitia containing predominantly FAP-positive cells at least suggest that they are highly proliferative (Figure S11). Taken together, our observations that *Pparg*$^{C/-}$ fibroblasts are actively contributing to collagen deposition and enlargement of aneurysm adventitia suggest that the regulatory role of PPARγ in fibroblasts has a direct impact on the overall vessel integrity in AAA.

Our *in vitro* study showed that PPARγ inhibition in MEFs, but not in VSMCs, dramatically attenuated expression of *Eln* and *Fbln5*. ChIP analysis in MEFs further confirmed a direct interaction between PPARγ and *Fbln5*. This PPARγ-interacting region is located in the introns of *Fbln5*, and a similar intronic regulation by PPARγ has been reported.[39] *FBLN5* expression was also reduced in the PPARγ-knockdowned HAoAFs, albeit to a lesser degree. It is worth noting that the effects of PPARγ knockdown on expression of *Eln* differ between MEFs and HAoAFs. Although species variation cannot be ignored, the response of embryonic fibroblasts may differ from that of adult primary vascular fibroblasts. Elastogenesis is restricted to a short period of embryonic and neonatal stages, and by the postnatal day 14, right after the deposition of elastin and assembly into extracellular fibers, the synthesis and production of elastic fibers are shut down rapidly. However, in the pathological condition, like AAA, adventitial fibroblasts encounter numerous stimulants, such as AngII and inflammatory cytokines. These stimulated fibroblasts may have a distinct regulatory program on elastic fiber components from fully differentiated, quiescent cells. Since we did not detect a direct interaction between PPARγ and *Eln*, the down-regulation of *Eln* by PPARγ antagonism in MEF may be mediated through an indirect mechanism. While the detailed regulation of *Fbln5* and *Eln* expression by PPARγ requires further investigation, PPARγ may be considered as a potential target for regulating elastogenesis in AAA therapy.

Perspectives

Our study of mice with varying *Pparg* expression indicates that quantitative variants causing decreased *Pparg* expression are a risk factor for AAA. Without advanced stimulations, more than 25% of normal PPARγ level is necessary to maintain elastic fiber components in the aorta and fibroblasts are vital for this action. Thus, this study highlights the importance of adequate PPARγ level in AAA treatment through orchestrating proper elastogenesis and preserving elastic fiber integrity. Importantly, new pharmacological interventions targeting PPARγ should be revisited in AAA therapy.

Supplementary Material

Refer to Web version on PubMed Central for supplementary material.

Acknowledgments

We thank Dr. Shaw-Jenq Tsai at Department of Physiology of National Cheng Kung University for critical suggestions and Yu-Tzu Chang for technical assistance.

Sources of Funding

This work was supported by grants from the National Science Council Taiwan (102-2321-B-006-007 and 101-2320-B-006-036), National Health Research Institutes (EX104-10231SI and EX105-10511SI), National Cheng Kung University Top-Notch Project, and National Institute of Health (HL42630).

References

1. Anjum A, von Allmen R, Greenhalgh R, Powell JT. Explaining the decrease in mortality from abdominal aortic aneurysm rupture. Br J Surg. 2012; 99:637–645. [PubMed: 22473277]
2. Kurosawa K, Matsumura JS, Yamanouchi D. Current status of medical treatment for abdominal aortic aneurysm. Circ J. 2013; 77:2860–2866. [PubMed: 24161907]
3. Ailawadi G, Eliason JL, Upchurch GR Jr. Current concepts in the pathogenesis of abdominal aortic aneurysm. J Vasc Surg. 2003; 38:584–588. [PubMed: 12947280]
4. Wagenseil JE, Mecham RP. Vascular extracellular matrix and arterial mechanics. Physiol Rev. 2009; 89:957–989. [PubMed: 19584318]
5. Jacob MP. Extracellular matrix remodeling and matrix metalloproteinases in the vascular wall during aging and in pathological conditions. Biomed Pharmacother. 2003; 57:195–202. [PubMed: 12888254]
6. Jones JA, Zavadzkas JA, Chang EI, Sheats N, Koval C, Stroud RE, Spinale FG, Ikonomidis JS. Cellular phenotype transformation occurs during thoracic aortic aneurysm development. J Thorac Cardiovasc Surg. 2010; 140:653–659. [PubMed: 20219212]
7. Jiang C, Ting AT, Seed B. Ppar-gamma agonists inhibit production of monocyte inflammatory cytokines. Nature. 1998; 391:82–86. [PubMed: 9422509]
8. Marx N, Schonbeck U, Lazar MA, Libby P, Plutzky J. Peroxisome proliferator-activated receptor gamma activators inhibit gene expression and migration in human vascular smooth muscle cells. Circ Res. 1998; 83:1097–1103. [PubMed: 9831704]
9. Gao DF, Niu XL, Hao GH, Peng N, Wei J, Ning N, Wang NP. Rosiglitazone inhibits angiotensin ii-induced ctgf expression in vascular smooth muscle cells - role of ppar-gamma in vascular fibrosis. Biochem Pharmacol. 2007; 73:185–197. [PubMed: 17074304]
10. Gaillard V, Casellas D, Seguin-Devaux C, Schohn H, Dauca M, Atkinson J, Lartaud I. Pioglitazone improves aortic wall elasticity in a rat model of elastocalcinotic arteriosclerosis. Hypertension. 2005; 46:372–379. [PubMed: 15967870]
11. Jones A, Deb R, Torsney E, Howe F, Dunkley M, Gnaneswaran Y, Gaze D, Nasr H, Loftus IM, Thompson MM, Cockerill GW. Rosiglitazone reduces the development and rupture of experimental aortic aneurysms. Circulation. 2009; 119:3125–3132. [PubMed: 19506106]
12. Hamblin M, Chang L, Zhang H, Yang K, Zhang J, Chen YE. Vascular smooth muscle cell peroxisome proliferator-activated receptor-gamma deletion promotes abdominal aortic aneurysms. J Vasc Surg. 2010; 52:984–993. [PubMed: 20630681]
13. Moran CS, Clancy P, Biros E, Blanco-Martin B, McCaskie P, Palmer LJ, Coomans D, Norman PE, Golledge J. Association of ppargamma allelic variation, osteoprotegerin and abdominal aortic aneurysm. Clin Endocrinol (Oxf). 2010; 72:128–132. [PubMed: 19438902]
14. Tsai YS, Tsai PJ, Jiang MJ, Chou TY, Pendse A, Kim HS, Maeda N. Decreased ppar gamma expression compromises perigonadal-specific fat deposition and insulin sensitivity. Mol Endocrinol. 2009; 23:1787–1798. [PubMed: 19749155]
15. Daugherty A, Manning MW, Cassis LA. Antagonism of at2 receptors augments angiotensin ii-induced abdominal aortic aneurysms and atherosclerosis. Br J Pharmacol. 2001; 134:865–870. [PubMed: 11606327]
16. Koch AE, Haines GK, Rizzo RJ, Radosevich JA, Pope RM, Robinson PG, Pearce WH. Human abdominal aortic aneurysms. Immunophenotypic analysis suggesting an immune-mediated response. Am J Pathol. 1990; 137:1199–1213. [PubMed: 1700620]
17. Trachet B, Fraga-Silva RA, Piersigilli A, Tedgui A, Sordet-Dessimoz J, Astolfo A, Van der Donckt C, Modregger P, Stampanoni MF, Segers P, Stergiopulos N. Dissecting abdominal aortic aneurysm in ang ii-infused mice: Suprarenal branch ruptures and apparent luminal dilatation. Cardiovasc Res. 2015; 105:213–222. [PubMed: 25538157]

18. Tsai YS, Xu L, Smithies O, Maeda N. Genetic variations in peroxisome proliferator-activated receptor gamma expression affect blood pressure. Proc Natl Acad Sci U S A. 2009; 106:19084–19089. [PubMed: 19884495]

19. Satoh K, Nigro P, Matoba T, O'Dell MR, Cui Z, Shi X, Mohan A, Yan C, Abe J, Illig KA, Berk BC. Cyclophilin a enhances vascular oxidative stress and the development of angiotensin ii-induced aortic aneurysms. Nat Med. 2009; 15:649–656. [PubMed: 19430489]

20. Daugherty A, Cassis LA. Mouse models of abdominal aortic aneurysms. Arterioscler Thromb Vasc Biol. 2004; 24:429–434. [PubMed: 14739119]

21. Kahari VM, Chen YQ, Bashir MM, Rosenbloom J, Uitto J. Tumor necrosis factor-alpha down-regulates human elastin gene expression. Evidence for the role of ap-1 in the suppression of promoter activity. J Biol Chem. 1992; 267:26134–26141. [PubMed: 1281483]

22. Nakachi Y, Yagi K, Nikaido I, Bono H, Tonouchi M, Schonbach C, Okazaki Y. Identification of novel ppargamma target genes by integrated analysis of chip-on-chip and microarray expression data during adipocyte differentiation. Biochem Biophys Res Commun. 2008; 372:362–366. [PubMed: 18489901]

23. Mithieux SM, Weiss AS. Elastin. Adv Protein Chem. 2005; 70:437–461. [PubMed: 15837523]

24. Liu X, Zhao Y, Gao J, Pawlyk B, Starcher B, Spencer JA, Yanagisawa H, Zuo J, Li T. Elastic fiber homeostasis requires lysyl oxidase-like 1 protein. Nat Genet. 2004; 36:178–182. [PubMed: 14745449]

25. Deng GG, Martin-McNulty B, Sukovich DA, Freay A, Halks-Miller M, Thinnes T, Loskutoff DJ, Carmeliet P, Dole WP, Wang YX. Urokinase-type plasminogen activator plays a critical role in angiotensin ii-induced abdominal aortic aneurysm. Circ Res. 2003; 92:510–517. [PubMed: 12600880]

26. Kanematsu Y, Kanematsu M, Kurihara C, Tsou TL, Nuki Y, Liang EI, Makino H, Hashimoto T. Pharmacologically induced thoracic and abdominal aortic aneurysms in mice. Hypertension. 2010; 55:1267–1274. [PubMed: 20212272]

27. Wilm B, Ipenberg A, Hastie ND, Burch JB, Bader DM. The serosal mesothelium is a major source of smooth muscle cells of the gut vasculature. Development. 2005; 132:5317–5328. [PubMed: 16284122]

28. Wasteson P, Johansson BR, Jukkola T, Breuer S, Akyurek LM, Partanen J, Lindahl P. Developmental origin of smooth muscle cells in the descending aorta in mice. Development. 2008; 135:1823–1832. [PubMed: 18417617]

29. Davis FM, Rateri DL, Balakrishnan A, Howatt DA, Strickland DK, Muratoglu SC, Haggerty CM, Fornwalt BK, Cassis LA, Daugherty A. Smooth muscle cell deletion of low-density lipoprotein receptor-related protein 1 augments angiotensin ii-induced superior mesenteric arterial and ascending aortic aneurysms. Arterioscler Thromb Vasc Biol. 2015; 35:155–162. [PubMed: 25395615]

30. Woldt E, Terrand J, Mlih M, Matz RL, Bruban V, Coudane F, Foppolo S, El Asmar Z, Chollet ME, Ninio E, Bednarczyk A, Thierse D, Schaeffer C, Van Dorsselaer A, Boudier C, Wahli W, Chambon P, Metzger D, Herz J, Boucher P. The nuclear hormone receptor ppargamma counteracts vascular calcification by inhibiting wnt5a signalling in vascular smooth muscle cells. Nat Commun. 2012; 3:1077. [PubMed: 23011131]

31. Gauthier A, Vassiliou G, Benoist F, McPherson R. Adipocyte low density lipoprotein receptor-related protein gene expression and function is regulated by peroxisome proliferator-activated receptor gamma. J Biol Chem. 2003; 278:11945–11953. [PubMed: 12551936]

32. Petrinec D, Liao S, Holmes DR, Reilly JM, Parks WC, Thompson RW. Doxycycline inhibition of aneurysmal degeneration in an elastase-induced rat model of abdominal aortic aneurysm: Preservation of aortic elastin associated with suppressed production of 92 kd gelatinase. J Vasc Surg. 1996; 23:336–346. [PubMed: 8637112]

33. Manning MW, Cassis LA, Daugherty A. Differential effects of doxycycline, a broad-spectrum matrix metalloproteinase inhibitor, on angiotensin ii-induced atherosclerosis and abdominal aortic aneurysms. Arterioscler Thromb Vasc Biol. 2003; 23:483–488. [PubMed: 12615694]

34. Xie X, Lu H, Moorleghen JJ, Howatt DA, Rateri DL, Cassis LA, Daugherty A. Doxycycline does not influence established abdominal aortic aneurysms in angiotensin ii-infused mice. PLoS One. 2012; 7:e46411. [PubMed: 23029514]

35. Meijer CA, Stijnen T, Wasser MN, Hamming JF, van Bockel JH, Lindeman JH. Pharmaceutical Aneurysm Stabilisation Trial Study G. Doxycycline for stabilization of abdominal aortic aneurysms: A randomized trial. Ann Intern Med. 2013; 159:815–823. [PubMed: 24490266]

36. Mosorin M, Juvonen J, Biancari F, Satta J, Surcel HM, Leinonen M, Saikku P, Juvonen T. Use of doxycycline to decrease the growth rate of abdominal aortic aneurysms: A randomized, double-blind, placebo-controlled pilot study. J Vasc Surg. 2001; 34:606–610. [PubMed: 11668312]

37. Henderson EL, Geng YJ, Sukhova GK, Whittemore AD, Knox J, Libby P. Death of smooth muscle cells and expression of mediators of apoptosis by t lymphocytes in human abdominal aortic aneurysms. Circulation. 1999; 99:96–104. [PubMed: 9884385]

38. Brokopp CE, Schoenauer R, Richards P, Bauer S, Lohmann C, Emmert MY, Weber B, Winnik S, Aikawa E, Graves K, Genoni M, Vogt P, Luscher TF, Renner C, Hoerstrup SP, Matter CM. Fibroblast activation protein is induced by inflammation and degrades type i collagen in thin-cap fibroatheromata. Eur Heart J. 2011; 32:2713–2722. [PubMed: 21292680]

39. Helledie T, Grontved L, Jensen SS, Kiilerich P, Rietveld L, Albrektsen T, Boysen MS, Nohr J, Larsen LK, Fleckner J, Stunnenberg HG, Kristiansen K, Mandrup S. The gene encoding the acyl-coa-binding protein is activated by peroxisome proliferator-activated receptor gamma through an intronic response element functionally conserved between humans and rodents. J Biol Chem. 2002; 277:26821–26830. [PubMed: 12015306]

Novelty and Significance

What Is New?

The critical amount of PPARγ for maintaining normal elastic waviness is above 50%, whereas the threshold level for elastic fiber breakdown is between 25% and 50%. Waviness loss of elastic fibers, which occurs early before the aneurysm develops, is attributable to PPARγ haploinsufficiency in conjunction with a moderate environmental insult.

PPARγ expression down to 25% (*Pparg*$^{C/-}$) in the aorta down-regulates the expression of vital elastic fiber components, elastin and fibulin-5. The regulatory role of PPARγ in elastogenesis takes place in fibroblasts by binding the genomic sequence of *Fbln5*.

What Is Relevant?

Our study highlights PPARγ as a vital regulator in AAA development. Thus, determination of PPARγ level/activity would be important for patients at a higher risk for developing AAA. Moreover, pharmacological intervention targeting PPARγ level/activity would be beneficial to preserve elastic fiber integrity during AAA initiation and development.

Summary

Our study underscores the importance of adequate PPARγ level in maintaining elastic fiber integrity though orchestrating proper expression of elastin and fibulin-5, further preventing from AAA development.

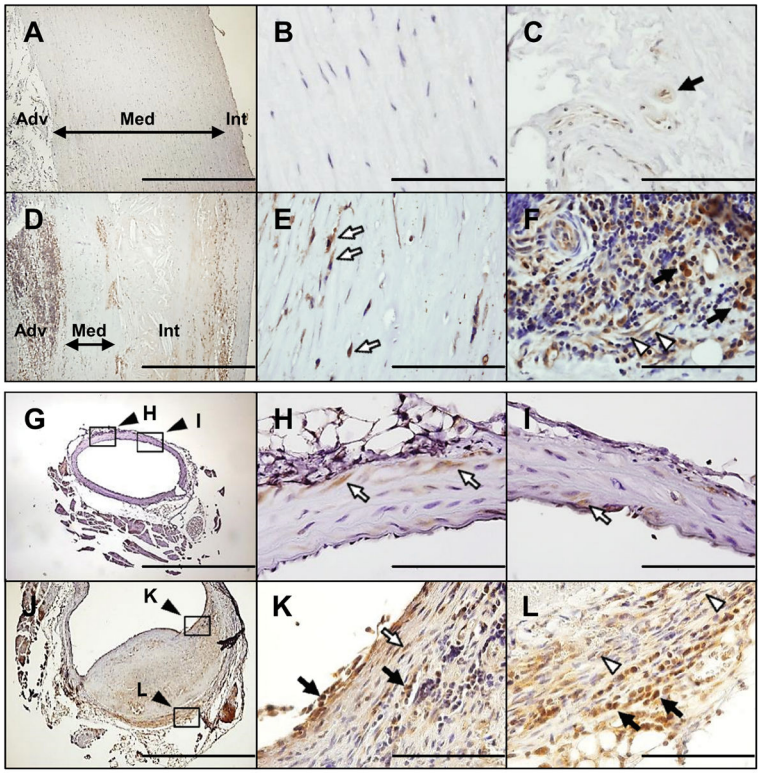

Figure 1.

Expression of PPARγ in human and mouse AAA. **A**–**F**, Immunohistochemical staining of PPARγ in normal human aorta (**A**–**C**) and human AAA (**D**–**F**). Filled arrows in (**C**) and (**F**) indicate cells resembling inflammatory cells. Open arrows in (**E**) resemble VSMCs. Open arrowheads in (**F**) indicate elongated endothelial cells or fibroblasts in or near microvessels. Int: intima; Med: media; Adv: adventitia. **G**–**I**, Normal AA of WT mice. Magnification of the black square in (**G**) is shown in (**H**) and (**I**). PPARγ expression is detected in some VSMCs of WT mice. **J**–**L**, AngII-induced dissecting AAA in WT mice. Section (**J**) shows prominent PPARγ expression in the inflammatory cells (filled arrows) of the luminal surface (**K**) and adventitia (**L**) as well as in VSMCs (open arrow in **K**), and fibroblasts (open arrowheads in **L**). Magnification of the black square is shown in the indicated picture. Scale bars in (**B**, **C**, **E**, **F**, **H**, **I**, **K**, and **L**) are 100 μm and in (**A**, **D**, **G** and **J**) are 1000 μm.

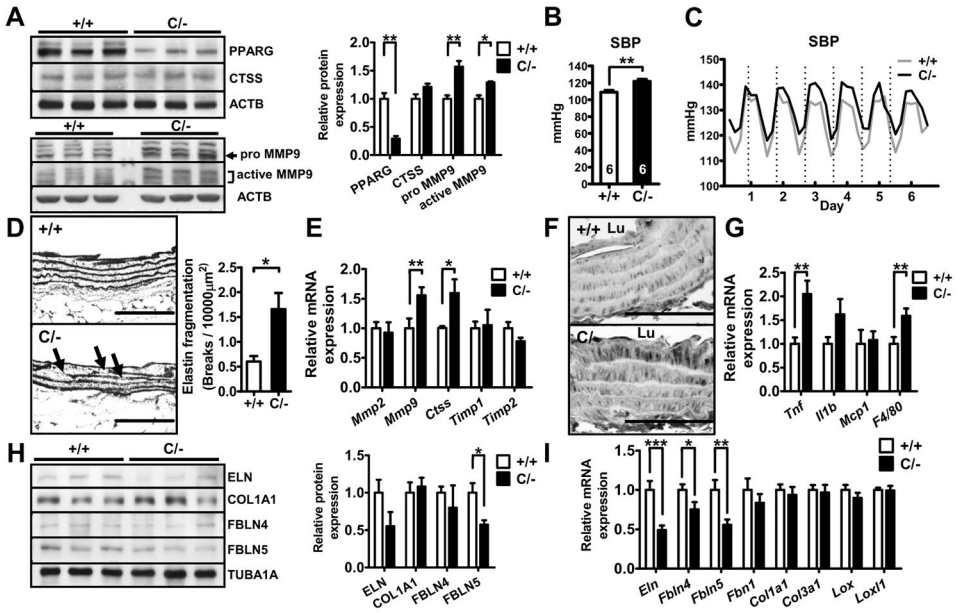

Figure 2.

Elastic fiber fragmentation and expression of elastic fiber components in *Pparg*$^{C/-}$ aorta. **A**, Immunoblot of PPARγ, cathepsin S and MMP-9 in the aorta (N=3 in each group). The relative intensities of the bands are indicated by densitometric quantification with WT. **B**, Tail-cuff and (**C**) telemetry systolic BP measurement in *Pparg*$^{+/+}$ and *Pparg*$^{C/-}$ mice. N=6 in (**B**) and 5 in (**C**). **D**, Representative images of the elastic network and quantification of elastic fiber breaks in the longitudinal section of aorta. Arrows indicate breaks in the elastic fiber. Numbers of breaks of elastic layers per 10,000 μm^2 are shown in the right (N=5 in each group). **E**, mRNA levels of elastolytic enzymes in *Pparg*$^{C/-}$ aorta are shown relative to the mean levels in *Pparg*$^{+/+}$ aorta as 1.0 (+/+ = 7, C/− = 6). **F**, Immunohistochemical staining of MMP-9 in the longitudinal section of aorta. Lu: lumen. **G**, mRNA levels of inflammatory cytokines and macrophage markers relative to the mean levels in *Pparg*$^{+/+}$ aorta as 1.0 (+/+ = 20, C/− = 16). **H**, Immunoblot and quantification of ECM components in the soluble fraction of aortic lysates (N=3 in each group) **I**, mRNA levels of ECM components (N=12–14 in each group).* P<0.05, ** P<0.01, and *** P<0.001. Scale bars in (**D**) are 100 μm and in (**F**) are 50 μm.

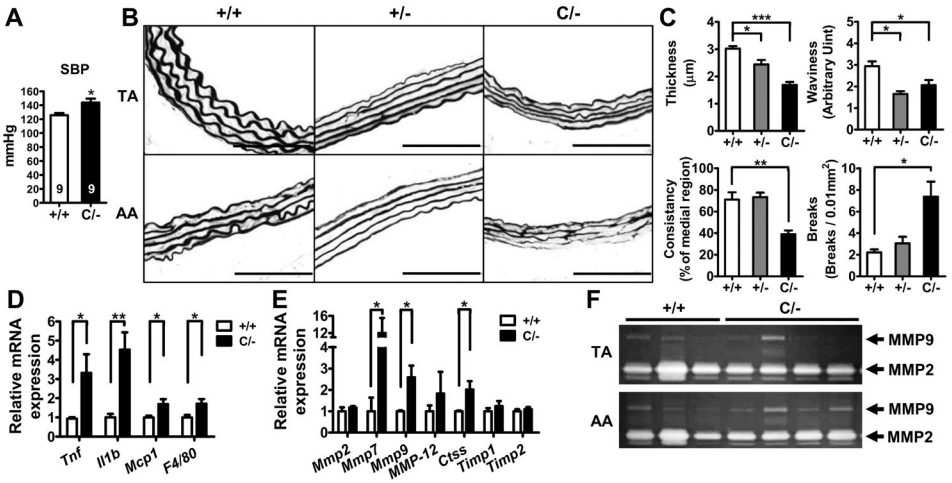

Figure 3.

Effects of moderate-dose AngII (500 ng/kg/min) infusion. **A**, Tail-cuff systolic BP measurement in AngII-infused *Pparg*$^{+/+}$ and *Pparg*$^{C/-}$ mice (N=9 in each group). **B**, Representative images of the elastic network in the TA and AA. Scale bars are 100 μm. **C**, Parameters of elastic fiber integrity, including thickness, waviness, consistency, and breaks of elastic lamellae, in the AA (+/+ = 5, +/− = 3, C/− = 7). *P<0.05, **P<0.01, and ***P<0.001 by one-way ANOVA with Tukey HSD test. **D** and **E**, mRNA levels for inflammatory mediators and for elastolytic proteases, respectively, in the aorta. Data are expressed relative to the mean in *Pparg*$^{+/+}$ aorta as 1.0 (N=5 in each group). *P<0.05 and **P<0.01 by Student's t-test. **F**, Gelatin zymography of protein lysate from TA and AA.

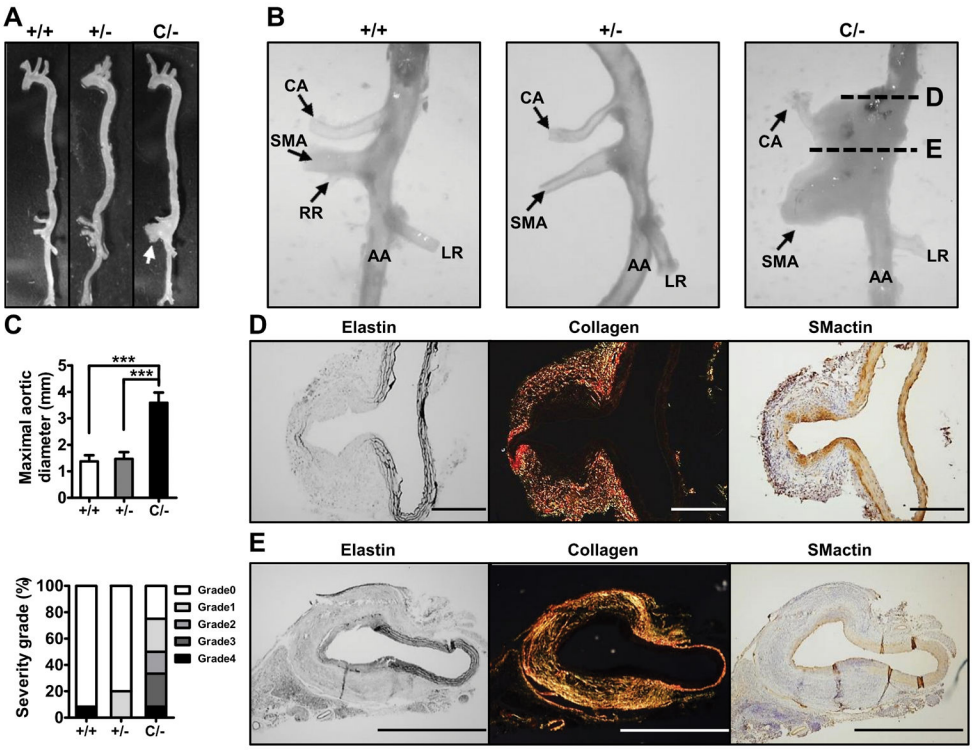

Figure 4.

Suprarenal aneurysms in high-dose AngII (1000 ng/kg/min) infused *Pparg*$^{C/-}$ mice. **A**, Representative photographs of the aorta. White arrow indicates aneurysm. **B**, Magnified view of AA region. CA: celiac artery. SMA: superior mesenteric artery. RR: right renal artery. LR: left renal artery. **C**, Maximal external aortic diameter and percentage of severity grade in AngII-infused mice (+/+ = 6, +/− = 5, C/− = 6). **D** and **E**, Elastin, collagen (PS red) staining and immunohistochemistry staining for SMactin of AA. ***P<0.001 by one-way ANOVA with Tukey HSD test. Scale bars in (**D**) are 200 μm and in (**E**) are 1000 μm.

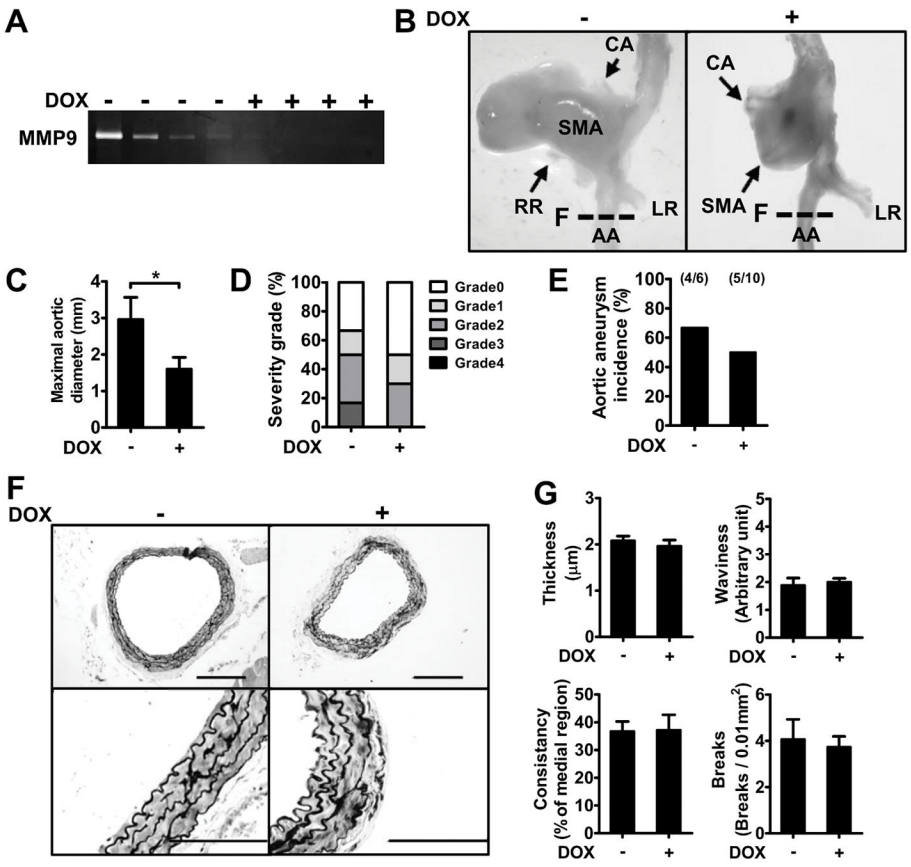

Figure 5.

Effects of MMP inhibition on AngII-infused *Pparg*$^{C/-}$ aneurysm. **A**, Gelatin zymography of protein lysates from AA. **B**, Representative photographs of the AAA. **C**, Maximal aortic diameter, (**D**) percentage of severity grade and (**E**) incidence of AAA in AngII-infused *Pparg*$^{C/-}$ mice. **F**, Representative images of the elastic network and (**G**) parameters of elastic fiber integrity in AA (N=5–6 in each group). Locations of sections in (**F**) were indicated by dash lines in (**B**). Scale bars are 200 μm in upper panels and 100 μm in lower panels of (**F**). *P<0.05.

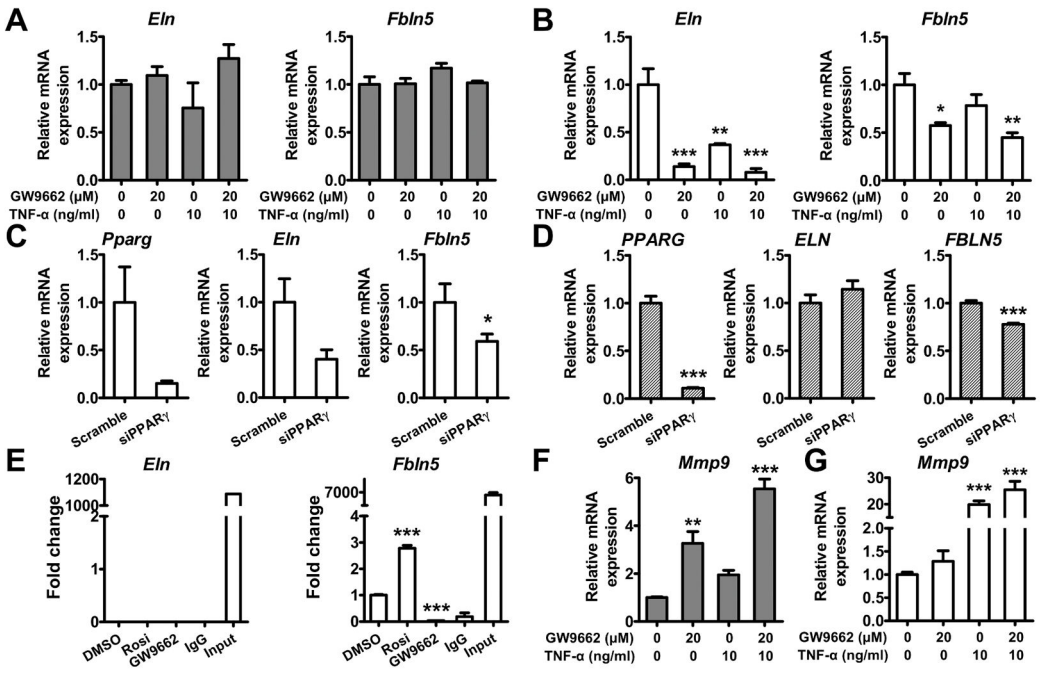

Figure 6.

Effects of PPARγ antagonism on expression of elastic fiber components. Expression of *Eln* and *Fbln5* after treatment with GW9662 or TNF-α in rat ASMCs (**A**, gray bars) and MEFs (**B**, white bars). N=3 in each group. **C**, Expression of *Pparg*, *Eln* and *Fbln5* in MEFs and (**D**) HAoAFs treated with scrambled siRNA or siRNA against PPARγ (siPPARγ). N=7–8 in each group. **E**, ChIP assay in MEFs. Sequences containing the potential PPARγ binding sites in *Eln* and *Fbln5* were amplified by real-time PCR. Rosi: rosiglitazone. Expression of *Mmp9* after treatment with GW9662, AngII, or TNF-α in rat ASMCs (**F**) and MEFs (**G**). **P*<0.05, ***P*<0.01, and ****P*<0.001 in (**A**–**B** and **E**–**G**) by one-way ANOVA with Tukey HSD test. **P*<0.05 in (**C** and **D**) by Student's *t*-test.

Table 1

Proteins involved in elastic fiber assembly and ECM organization.

Protein description	Ratio (C/− / +/+)	Quantifiable peptides	Identified peptides	Biological process
Fibulin-5	0.61	7	9	Elastic fiber assembly
Periostin	0.72	8	23	ECM organization
Elastin	0.82	7	11	Elastic fiber assembly
Collagen alpha-2(VI) chain	0.84	8	21	ECM organization
Fibrillin-1	0.84	7	40	Elastic fiber assembly
Decorin	0.85	3	8	ECM organization
Lysyl oxidase homolog 1	0.87	7	15	Elastic fiber assembly
Fibronectin	0.90	12	35	ECM organization
Basement membrane-specific heparan sulfate proteoglycan core protein	0.92	8	37	ECM organization
Collagen alpha-1(VI) chain	0.95	4	16	ECM organization
Collagen alpha-1(I) chain	1.00	6	8	ECM organization
Collagen alpha-2(I) chain	1.09	4	7	ECM organization

Identified peptides: number of peptides with MASCOT individual ion score above 20.

Quantifiable peptides: number of Identified peptides with quantitation ratio (C/− versus +/+).

N=5 in each group.